Int. J. Electrochem. Sci., 14 **(2019)** 8720 – 8732, doi: 10.20964/2019.09.10

International Journal of
ELECTROCHEMICAL
SCIENCE
www.electrochemsci.org

Service Life Assessment of Lead and its Alloy Anodes During Zinc Electrowinning

Chang-jiang Yang[*], *Lv-xing Zhao*, *Xu Zhang*

Faculty of Metallurgical and Energy Engineering, Kunming University of Science and Technology, Kunming 650093, P. R. China
[*]E-mail: chemdut@163.com, yangc@kmust.edu.cn

Received: 2 May 2019 / *Accepted:* 20 June 2019 / *Published:* 31 July 2019

Lead (Pb) and its alloy anodes are widely used in the process of zinc electrowinning. It is important, yet difficult, to evaluate the service life of different anodes with varying components. In this work, electrochemical accelerated corrosion tests were investigated for the prediction of service life. Corrosion of pure Pb, Pb-0.75 wt.% Ag, and Pb-0.287 wt.% Ag-0.914 wt.% Ca anodes were investigated in the simulated electrolyte with and without manganese ion. Corrosion potentials, polarizing resistances, corrosion currents, and current efficiencies of the three typical anodes are further discussed. The semi-empirical relationship between corrosion rate and current density was suggested to obtain consumption rates of Pb-based anodes by rapid evaluation in the bench-scale experiments. Both the service life and the energy efficiency can be acquired according to the expression obtained.

Keywords: Corrosion rate; Pb; Anode; Zinc electrowinning

1. INTRODUCTION

The electrowinning (EW) processes of many metals, such as Zn, Cu, Co, Mn, and Ni, with Pb-based anodes have been used in the electrometallurgical industry for tens of decades[1]. At present, 85% of the world's Zn is produced by the EW process and lead–silver alloys are used as the primary anodes, which are also predominantly used for other sulphate-based aqueous systems[2]. The survival of Pb anodes is due to their cost efficiency and long-term stability at high current densities and in aggressive environments; however, their drawbacks include high overpotential and the possibility of cathode contamination. Many elements, such as Sb, Ca, Ag, and Sn, have been chosen to alter the electrochemical performance of Pb by alloying[3]. The service life of Pb anodes is usually 1–2 years in practice, depending mainly on lead consumption[4, 5]. The corrosion properties are critical to assess Pb anodes to be utilized in factories. Corrosion rates depend on many operating parameters including not only alloying elements but also acid concentration, temperature, current density, preconditioning, and

presence of Mn^{2+}, Cl^{-}, and Zn^{2+}, etc.[3, 4, 6]. Fortunately, these environmental factors are almost stable during the typical zinc electrowinning process.

Numerous investigations have focused on the corrosion resistance of Pb anodes by weight loss or electrochemical methods[5, 7, 8]. Potentiodynamic polarization measurement can determine the corrosion parameters, such as corrosion current, corrosion potential, and polarization resistance[2, 9]. Electrochemical impedance spectroscopy provides in-situ information of corrosion kinetics and mechanism of reactions[10, 11]. Electrochemical noise measurements have been used to detect corrosion by calculating the resistance noise[12]. These parameters of corrosion rates are usually obtained for Pb anodes at open-circuit potential or during current interruption. Usually, gravimetric methods can be used to determine corrosion rates of Pb alloys under harsh working conditions[13, 14].

There is almost no literature devoted to evaluating the service life of Pb-based anodes from bench-scale experiments. It is also very difficult to compare the measuring results of different type Pb anodes due to varied conditions and methods of tests[2, 10, 14]. The aim of this work was to explore a method to assess the service life of Pb-based anodes in the zinc electrowinning process based on corrosion rates. An electrochemical accelerated corrosion test was employed as a rapid method to acquire corrosion rates under simulated industrial conditions of zinc electrowinning.

2. MATERIALS AND METHODS

2.1 Sample preparation

Three typical Pb-based anodes were used for the assessment of corrosion. Pure Pb foils were purchased from Alfa Aesar with purities >+99.9 wt% (written as "Pure Pb", hereafter). Pb- 0.75 wt.% Ag alloy and Pb- 0.287 wt. % Ag-0.914 wt.% Ca alloy were commercial products supplied by the Kunming Hengda Technology and Mengzi Mine Smelting Company, respectively (abbreviated hereafter as "PbAg" and "PbAgCa", respectively). All samples were wet ground on abrasive papers of 600#, 800#, 1200#, and 2000#, and ultrasonically cleaned in ultra-pure water (>18 MΩ, Hitech Instruments), ethanol, and acetone sequentially. Then, they were dried by a high-purity nitrogen stream. The specimens were cut to fit a polytetrafluoroethylene (PTFE)-coated flat specimen holder (AIDAhengsheng, JJ210) with a 1 cm^2 area exposure to the test solution.

2.2 Solution preparation

All chemicals were analytical reagent (AR) grade and obtained from the Sinopharm Chemical Reagent Company without further purification. The composition of the electrolyte solution was similar to that used in a zinc electrowinning plant. The basic electrolyte was 150 g/L(≈ 1.53 M) H_2SO_4 + 60 g/L(≈ 0.92 M) Zn^{2+}($ZnSO_4$), and the other solution was 150 g/L(≈ 1.53 M) H_2SO_4 + 60 g/L(≈ 0.92 M) Zn^{2+}($ZnSO_4$) + 2 g/L(≈ 0.036 M) Mn^{2+}($MnSO_4$). To suppress zinc deposition on a Pt cathode, 5 mg/L of antimony (as antimony potassium tartrate) was added to the electrolyte[13]. The temperature of the solution during the experiment was maintained at 36±1℃ in a water bath (Yuhua, DF-101S).

2.3 Measurements

2.3.1. Weight loss tests

The electrochemical accelerated corrosion tests were performed gravimetrically in a conventional two-electrode system, with a 4 cm^2 area Pt sheet as the cathode. The cleaned specimens were dried at 105℃ for 1 hour and weighed using a balance with an accuracy of 0.1mg (Mettler Toledo). Then, they were placed in the electrolyte solution and used as the anode under a constant current (Good Will Instrument, GPD-2303S). The bulk of the electrolyte was kept as 1 L by both condensing water vapor and frequent addition of pure water due to water splitting. The solution was rigorously stirred with a Teflon stir bar at about 1000 r/min to minimize the attachment of corrosion products on the surface of the anode. The current densities were set at 500, 2500, 5000, 7500, and 10000 A/m^2 for 20 hours, unless otherwise stated. A time of 20 hours was chosen because Newnham[13] and Hine[15] observed that the corrosion rates of Pb anodes were equivalent for different periods during electrochemical accelerated tests. At the end of the tests, the samples were rinsed with pure water, and any build-up of lead oxide or manganese dioxide was carefully removed with soft cloths or rubber. It has been reported that the mass of the lead dioxide layer is negligible compared to the overall weight loss[13]. Next, the sample was ultrasonically cleaned in ultra-pure water, ethanol, and acetone sequentially, dried at 105℃ for 1 hour, and weighed after cooling to a constant weight in a desiccator. The determination was repeated three times at the same condition, and the average of these values was used for analysis.

2.3.2. Potentiodynamic polarization

A computer controlled Versastat 3 potentiostat/galvanostat (Ametek, USA) performed electrochemical characterizations with VersaStudio software. A three-electrode system was used in simulated zinc electrowinning electrolyte solution which consisted of 60 g/L Zn^{2+} and 160 g/L H_2SO_4. The temperature of the electrolyte was maintained at 36℃ by a thermostatic water bath (Yuhua, DF101). Three typical materials were used as the working electrodes, and a platinum sheet and a mercury/mercurous sulphate electrode (in saturated K_2SO_4) (MSE, 0.652V vs. NHE) were used as the counter electrode and the reference electrode, respectively. Pre-treatment of the anodes using consecutive multiple cyclic voltammetry (CV) was performed with 30 runs from 0.35V to 1.55V (vs. MSE) with a sweep rate of 30 mV/s to obtain consistent and reproducible results. The potentials in this paper were vs. MSE, unless stated otherwise. All overpotentials (η) for the oxygen evolution reaction (OER) from H_2O were calculated by the following equation:

$$\eta = E(NHE) - E'_{H_2O/O_2} - j \times R_s \quad (1)$$

where, E'_{H_2O/O_2} is the thermodynamic oxygen evolution potential in an acid, defined as 1.229-0.059×pH(V), and R_s is the electrolyte resistance which is determined by the electrochemical impedance.

The linear sweeping voltammograms (LSVs) were recorded by linear sweep of the potential at a sweep rate of 1 mV/s from 0.35 V to 1.75 V in the region of oxidations of anodes and oxygen evolution. The slow sweep rate was chosen to minimize any pseudo-capacitance to reach the steady-state current density. The solution was rigorously stirred with a Teflon stir bar to keep the reaction in the activation-

controlled region to avoid mass transport effects. Tafel plots were obtained by plotting the overpotential (η) vs. Log (j) (x-axis) from the LSVs, where j is the current density based on the geometrical surface area of the electrode.

2.4 Physical characterization

The morphology of the surface of the anode after the corrosion experiment was investigated using scanning electron microscopy (SEM, Shimadzu, EMPA-1720). The corrosion products suspended in the electrolyte were filtered and separated with a microporous membrane (0.2 μm) and dried in a vacuum oven. The morphology and atomic ratios of the powders were determined with an electron microprobe (Shimadzu, EMPA-1720). The content of lead sulphate in the powder was calculated from the sulphur quantity determined by a C/S analyser (Eltra, CS 2000). X-ray diffraction (XRD, Rigaku, D/Max 2200) using a Cu Kα (1.54056A) target was carried out with a scanning rate of 8°/min with a step of 0.02°. Raman spectra were recorded from the corrosion powders at room temperature using a Renishaw inVia Raman microscope with a helium laser at 514.5 nm. Each sample was subjected to 60 s over the range of 100−1500 cm^{-1} with a power of 1 mW to avoid laser heating of the specimen.

3. RESULTS AND DISCUSSION

3.1 Corrosion characterization

The morphologies of both Pure Pb and PbAg after the accelerated corrosion tests at a current of 500 A/m^2 in 150 g/L H_2SO_4 + 60 g/L Zn^{2+} solution for 20 hours are shown in Figure1. Both show a loose and porous oxide appearance and significant intergranular corrosion. These pores and crevices play critical roles in ion transportation, resulting in corrosion of the bulk metal. There are less defects on the surface of the PbAg anode than on the Pure Pb, and the oxide particles on the surface of the PbAg anode are smaller than those of Pure Pb, which can provide more corrosion resistance. Ag can close the pores in $PbSO_4$ and coarsen the grain size and structure[16], which is of imminent importance for the rate of corrosion in industrial electrolytes[17].

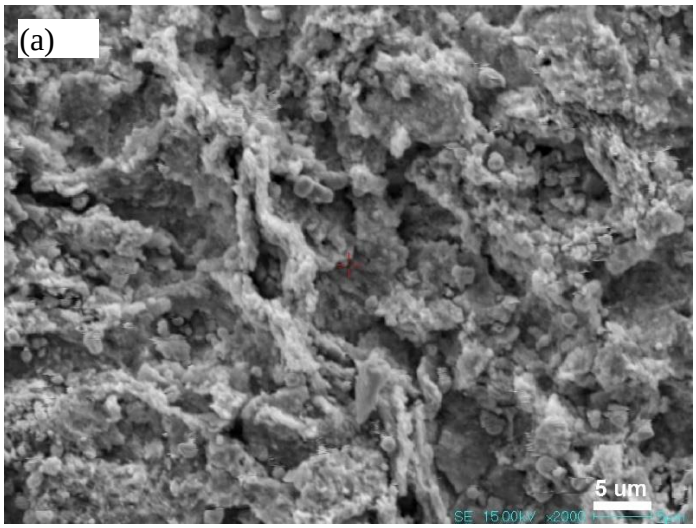

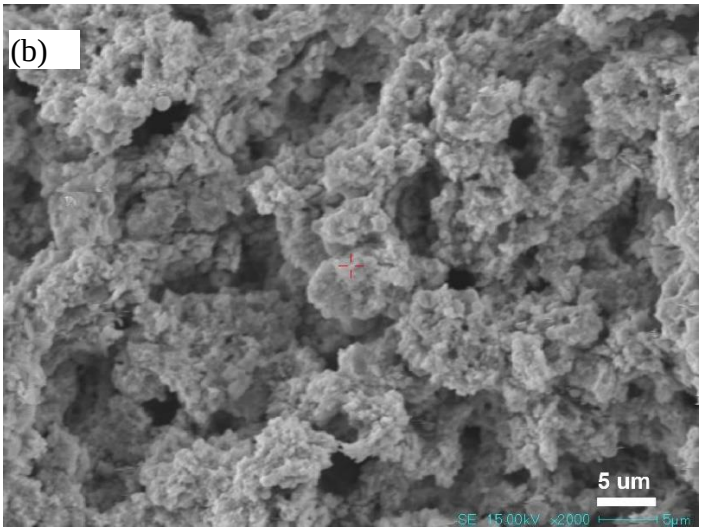

Figure 1. The morphologies of Pure Pb(a) and PbAg (b) after corrosion tests at a current of 500 A/cm^2 in 150 g/L H_2SO_4 + 60 g/L Zn^{2+} electrolyte for 20 hours.

Since Pb^{2+} concentrations in electrolytes are around 2.5 mg/L, without the Mn ion, and 1.3 mg/L with the addition of 1 g/L Mn ion[4], most corrosion products will accumulate in the electrolyte as slime due to exfoliation of drastic oxygen bubbles on the surface of the anode. The particles in the electrolyte from experiments with Pure Pb after the corrosion tests at a current of 10000 A/m^2, both in a basic solution of 150 g/L H_2SO_4 + 60 g/L Zn^{2+} and in a basic solution with the addition of 2 g/L Mn^{2+} for 20 hours, were collected. The XRD patterns are shown in Figure 2. The powders from the solution without Mn consisted of 92.4 wt.% PbO_2 and 7.6 wt.% $PbSO_4$, based on analysis of XRD data and C/S analyser data. The particles in solution with the addition of Mn contained 92.7 wt.% MnO_2, 6.7 wt.% $PbSO_4$, and 0.6 wt.% PbO_2, which were calculated by combining the energy dispersive spectrometer (EDS) and C/S analyser results. It is indicated that there is preferential oxidation of Mn^{2+} during oxygen evolution, and the dissolving of Pb is reduced, which leads to slow consumption of anodes. These results are consistent with analysis of the corrosion layer in previous literature[4]. In zinc electrowinning plants, these corrosion products will build up on the surface of the anodes, forming slime that must be removed frequently because of overpotential and contamination of the cathode.

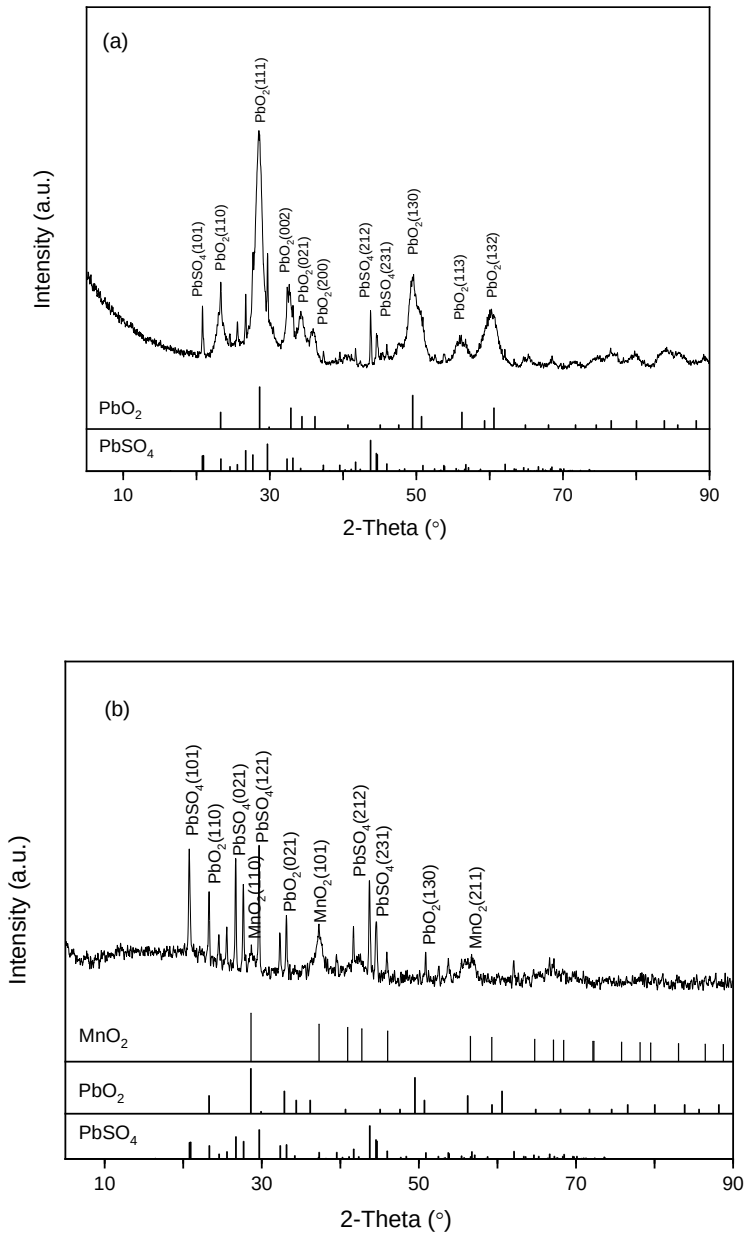

Figure 2. XRD patterns of powders of corrosion products from Pure Pb after corrosion tests at a current of 10000 A/m^2 in 150 g/L H_2SO_4 + 60 g/L Zn^{2+} electrolyte (a) and in the electrolyte with the addition of 2 g/L Mn^{2+} (b) for 20 hours.

The Raman spectra in Figure 3 show that the strong sulphate bands are clearly visible[18]. A broad band at ~450 cm^{-1} is associated with the O−S−O bending vibration, and lead sulphate often has two sharp bands in that region, at 439 and 451 cm^{-1}. The 970 and 1123 cm^{-1} bands are characteristic of the SO_4 symmetric stretching vibration[19]. Since PbO_2 is very sensitive to irradiation and degrades immediately, it is difficult to obtain a Raman spectrum from PbO_2[20]. The weak, broad bands at 100−200 cm^{-1} are due to suboxides of lead formed by laser-induced decomposition of PbO_2. The very broad band at 542 cm^{-1} is readily attributed to Pb_3O_4, which formed from PbO_2[20]. It is also known

that bands in the high-frequency region, ~570 and ~630 cm^{-1}, belong to the MnO_2, which originate from breathing vibrations of the MnO_6 octahedra within a tetragonal hollandite-type framework[21, 22].

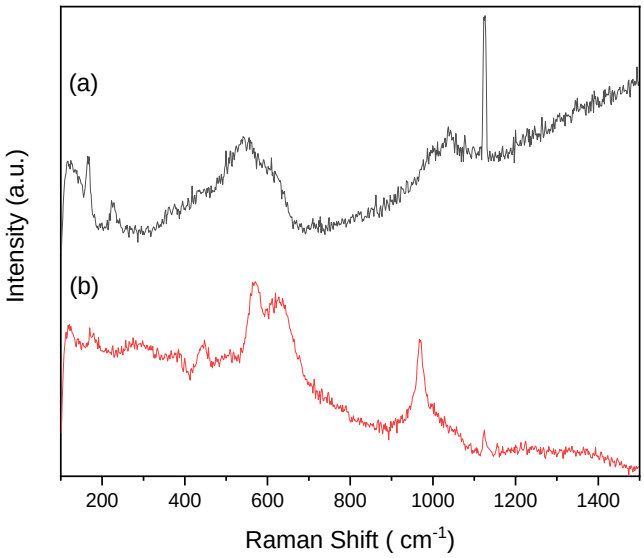

Figure 3. Raman spectra of powders of corrosion products from Pure Pb after corrosion tests at a current of 10000 A/m^2 in 150 g/L H_2SO_4 + 60 g/L Zn^{2+} electrolyte (a) and in the electrolyte with the addition of 2 g/L Mn^{2+} (b) for 20 hours.

The SEM images of powders of the corrosion products are shown in Figure 4. The powders in Figure 4a formed in 150 g/L H_2SO_4 + 60 g/L Zn^{2+} solution, are composed of flaky PbO_2 particles with diameters of 5 μm and $PbSO_4$ particles with diameters less than 1 μm. The powders in Figure 3b from the solution with the addition of Mn are aggregation of MnO_2 particles with diameters that are tens of nanometer. The results agree well with an early study[4] that showed that anode slime is mostly suspended with diameters less than 20 μm. Compared with the literature[4], it can be concluded that the particle sizes are much more uniform and smaller at high anodic current densities.

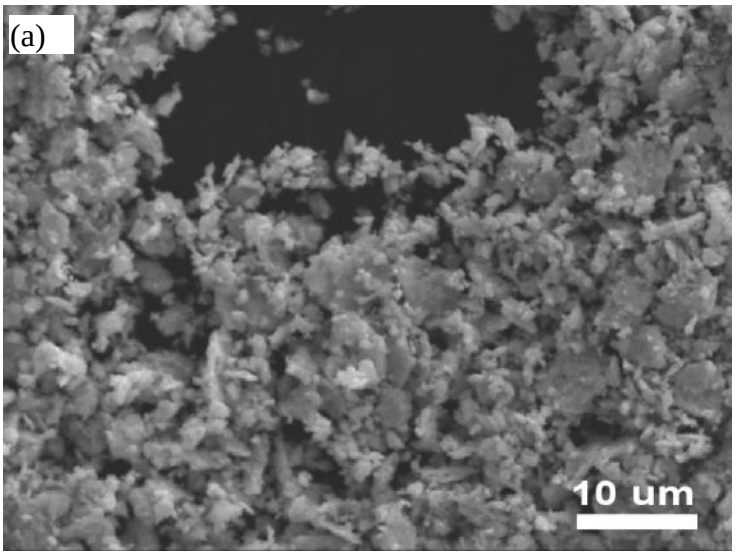

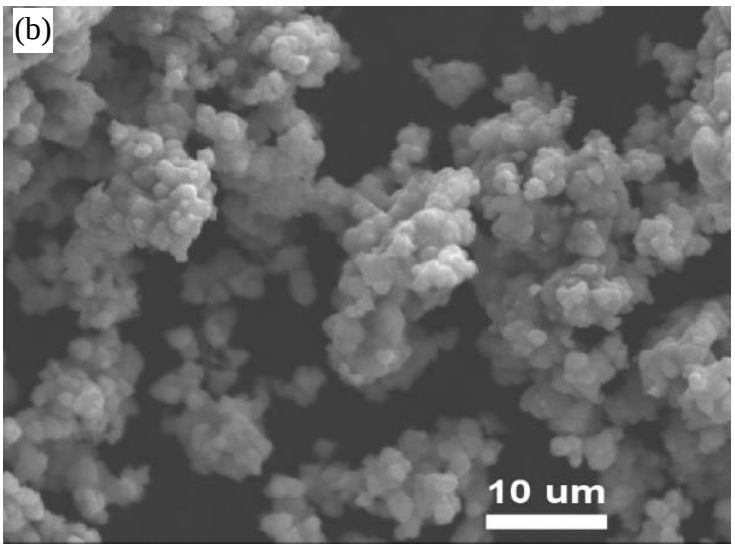

Figure 4. SEM micrographs of powders of corrosion products from Pure Pb after corrosion tests at a current of 10000 A/m^2 in 150 g/L H_2SO_4 + 60 g/L Zn^{2+} electrolyte (a) and the electrolyte with the addition of 2 g/L Mn^{2+} (b) for 20 hours

3.2 Electrochemical polarization analysis

LSVs recorded for the Pure Pb, PbAg and PbAgCa at sweep rate of 1 mV/s in 150 g/L H_2SO_4 + 60 g/L Zn^{2+} electrolyte are shown in Figure 5. The polarization curves of the three anodes are similar. Both corrosion and Tafel parameters ware shown in Table 1, and obtained by the Tafel extrapolation technique at selected potential ranges. The corrosion currents (I_{corr}) were calculated based on the "Stern-Geary" expression[23], as follows:

$$I_{corr} = \frac{b_a|b_c|}{b_a+|b_c|} \times \frac{R_p}{2.3} \qquad (2)$$

where R_p is the polarization resistance at E_{corr} and b_a and b_c are the Tafel constants. The corrosion potentials of Pb-based anodes are higher than those of Pure Pb thanks to the high equilibrium potential of Ag. The corrosion currents of Pb-alloy anodes result from bimetallic corrosion between Pb and the alloying elements. In the overpotential range of oxygen evolution, the anodic Tafel slopes of those anodes are all about 170 mV/dec, which indicate that the mechanism of oxygen evolution on the surface is the same. All exchange current densities (j_0) are of the same order of magnitude as a previous report[4]. It is also reasonable that the potentials have a linear relationship with the logarithm of current densities, as follows:

$$E = C_1 \times \log(j) + C_2 \qquad (3)$$

Where E and j are the potential and current of the electrode during oxygen evolution, respectively, and C_1 and C_2 are constants.

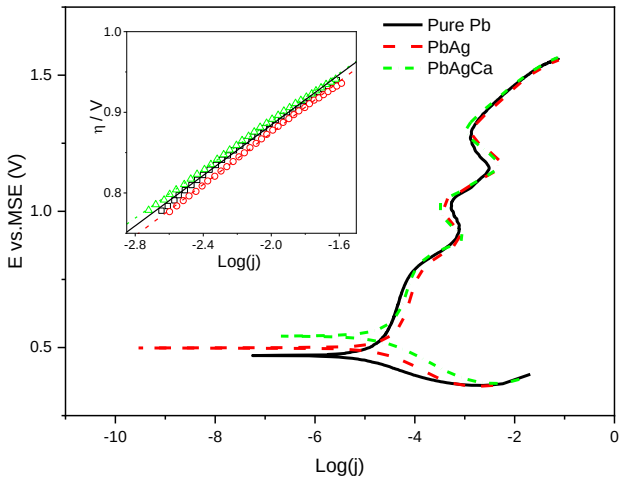

Figure 5. LSVs recorded for the Pure Pb(—), PbAg (---), and PbAgCa(-•-) at sweep rate of 1mV/s in in 150 g/L H_2SO_4 + 60 g/L Zn^{2+} electrolyte at 36℃. Inset: The Tafel fitting in the overpotential range of oxygen evolution.

Table 1. Corrosion and Tafel parameters evaluated from linear sweeping voltammograms (LSVs).

Specimens	Corrosion			Tafel	
	E_{corr} (V)	I_{corr} (A/cm^2)	R_p (Ω cm^2)	Anodic slope (mV/dec)	j_0 (A/cm^2)
Pure Pb	0.470	6.17x10^{-6}	2087	156	2.11x10^{-8}
PbAg	0.498	1.78x10^{-5}	1116	160	3.47x10^{-8}
PbAgCa	0.542	1.97x10^{-5}	1198	160	3.76x10^{-8}

3.3 Evaluation based on corrosion rates

The corrosion rates (CR) of all anodes were calculated in accordance with ASTM G1 and G31, as follows:

$$\mathrm{CR} = \frac{K \times W}{A \times t \times \rho} \qquad (4)$$

where CR=corrosion rate in mm/y, K=87600, W=mass loss in g (to the nearest 0.1 mg), t=time of accelerated test in hours, A=area in cm^2, and ρ=density in g/cm^3.

The corrosion rates of the three anodes as functions of current densities are shown in Figure 6. The longitudinal coordinate is a logarithm of W, and the horizontal coordinate is a logarithm of current density. It can be seen that the corrosion rates have nothing to do with the corrosion current (I_{corr}) or polarization resistance (R_p) as a consequence of the varying potential ranges and different reactions. It is evident that there is a linear relationship between the corrosion rate and current density in the logarithmic coordinate for the three anodes. It agreed well with the report of Nidola [24] and Hine[15], who showed that the corrosion rates of Pb anodes containing 0.1−5.0 wt.% Ag increased with current densities of 2500−10000 A/m^2 for 100 hours. In other words, the log(CR) is proportional to log(j), as in the following expression:

$$\log(\mathrm{CR}) = C_3 \times \log(j) + C_4 \qquad (5)$$

where CR and *j* are the corrosion rate and current density of electrodes, respectively, and C_3 and C_4 are constants.

Combing Eq. (3) and (5) gives the following,

$$\log(\mathrm{CR}) = C_5 \times E + C_6 \qquad (6)$$

where C_5 and C_6 are constants. The relationship between corrosion rate and potential (*E*) in Eq.(6) was also found in a previous study[25].

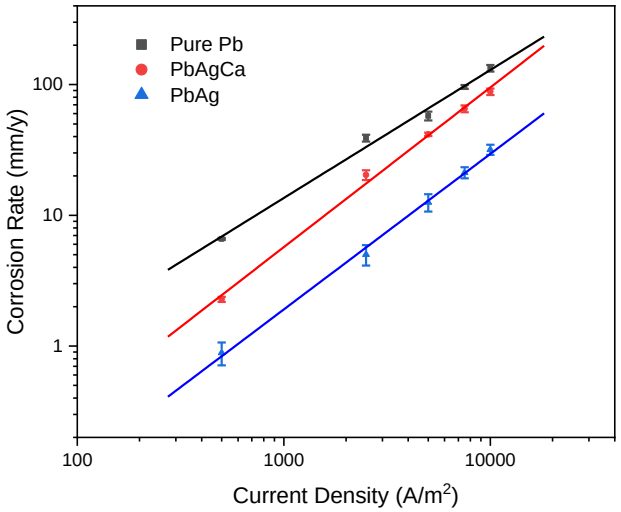

Figure 6. Corrosion rates of the Pure Pb(□), PbAgCa (○) and PbAg (△) as a function of current density in 150 g/L H_2SO_4 + 60g/L Zn^{2+} electrolyte at 36℃.

Table 2. Current efficiencies (CE) of Pb-based anodes in the electrolyte with and without Mn^{2+}.

Current density (A/m^2)	Pure Pb	PbAg	PbAgCa	Pure Pb	PbAg	PbAgCa
	CE in the basic electrolyte* (%)			CE with the addition of Mn^{2+} (%)		
500	99.56	99.94	99.85	99.62	99.97	99.94
2500	99.48	99.93	99.73	99.50	99.96	99.91
5000	99.61	99.92	99.72	99.56	99.95	99.88
7500	99.57	99.91	99.71	99.57	99.95	99.86
10000	99.60	99.89	99.70	99.58	99.94	99.85

*The basic electrolyte is a solution of 150 g/L H_2SO_4 + 60 g/L Zn^{2+}.

Current efficiency (CE, %) is usually used in the electrowinning industry and is defined as the following: $1\text{-}j_{pb}/j_{app}$, where j_{pb} is the corrosion current density of Pb in forming Pb^{2+}, while j_{app} is the applied current on the anode. The corrosion current density (j_{pb}) is calculated as follows:

$$j_{Pb} = \frac{F \times W}{A \times t \times M} \qquad (7)$$

where j_{pb} is the corrosion current density in A/m^2, F = 96485(Faraday's constant) in C/mol, W = the mass loss in g(to the nearest 0.1mg), t = the time of the accelerated test in seconds, A = the area in m^2, M = the molecular weight in g/mol.

Current efficiencies of all anodes are shown in Table 2. The current efficiencies of PbAg anodes are more than 99.9% and the highest among the three anodes. With increases in applied current density, the current efficiencies of both PbAg and PbAgCa were reduced slightly, while the current efficiencies of Pure Pb fluctuated in the range of 99.48−99.62%. The reason may be that Pb alloying with Ag and Ca elements is related to changes in the structure of the PbO_2 layer and decreased lifetime of the hydroxyl radical intermediate, which can reduce oxidation of the Pb substrate[26].

3.4 Impact of Mn^{2+} on the relationship between the corrosion rate and current density

The corrosion rates of the three anodes in the electrolyte with the addition of 2 g/L Mn^{2+} as a function of current densities are shown in Figure 7. Although all corrosion rates of the anodes decreased because of MnO_2 formation on the surface as a catalyst and a protecting layer[27], there is still an almost perfect linear relationship between log(CR) and log(*j*), with the adjusted R^2 larger than 0.992.

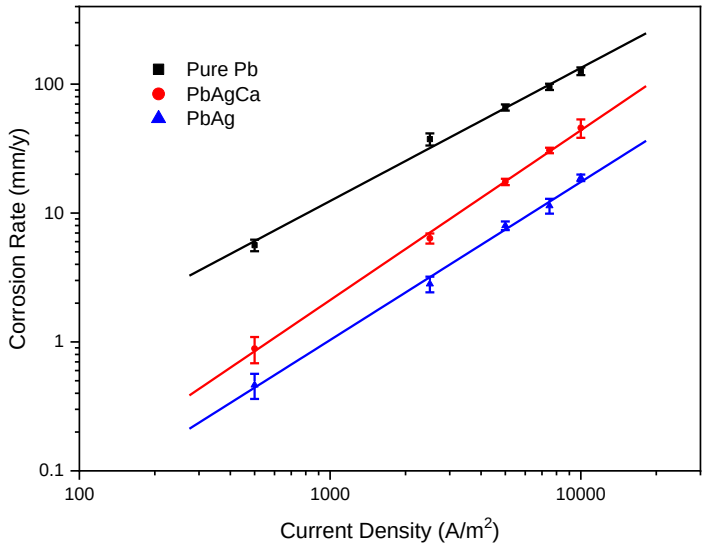

Figure 7. Corrosion rates of the Pure Pb(□), PbAgCa (○) and PbAg (△) as a function of current density in 150 g/L H_2SO_4 + 60 g/L Zn^{2+} + 2 g/L Mn^{2+} electrolyte at 36℃.

Therefore, we can assess the service life of lead and its alloy anodes based on Eq. (5) through electrochemical accelerated corrosion tests. Usually, weight loss tests of anodes from lead and its alloys under zinc electrowinning need to be more than one thousand hours to obtain reliable results[5]. Actually, we can accelerate the corrosion tests at very high current densities in a short time period and deduce the corrosion rate (CR_0) at any current density. Then, the service life of a fresh anode with a thickness of L_0 can be determined as $L_0/(2\ CR_0)$, in theory, assuming uniform corrosion.

4. CONCLUSIONS

To our knowledge, this is the first assessment of the service life of lead and its alloy anodes based on the electrochemical accelerated corrosion test. Electrochemical measurements and weight loss tests were employed to investigate the corrosion potentials, polarizing resistances, corrosion currents and current efficiencies of the pure Pb anode and two typical commercial Pb-alloy anodes. An important expression between corrosion rate and applied current during oxygen evolution is suggested. From the semi-empirical relationship between corrosion rate and current density, rapid evaluation of Pb-based anodes can be conducted in the bench-scale experiments. The results can also be used to compare different anodes on not only corrosion rates but also energy efficiency by the slopes and intercepts.

ACKNOWLEDGEMENTS
This work was financial supported by the National Natural Science Foundation of China [grant No.51664040], the Analysis and Testing Foundation of Kunming University of Science and Technology [grant No. 2019T20080042].

References

1. K. I. Popov, S. S. Djokić and B. Grgur, Fundamental Aspects of Electrometallurgy, Springer, (2002).
2. S. Wang, X.-y. Zhou, M. Chi-Yuan, B. Long, H. Wang, J.-J. Tang and J. Yang, *Hydrometallurgy*, 177 (2018) 218.
3. A. Mirza, M. Burr, T. Ellis, D. Evans, D. Kakengela, L. Webb, J. Gagnon, F. Leclercq and A. Johnston, *J.South.Afr.Inst.Min.Metall.*, 116 (2016) 533.
4. C. Zhang, N. Duan, L. Jiang, F. Xu and J. Luo, *Environ. SCi. Pollut. R.*, 25 (2018) 11958.
5. I. Ivanov, Y. Stefanov, Z. Noncheva, M. Petrova, T. Dobrev, L. Mirkova, R. Vermeersch and J. P. Demaerel, *Hydrometallurgy*, 57 (2000) 109.
6. L. Cifuentes and D. Pino, *Corros. Eng. Sci. Techn.*, 44 (2009) 474.
7. I. Ivanov, Y. Stefanov, Z. Noncheva, M. Petrova, T. Dobrev, L. Mirkova, R. Vermeersch and J. P. Demaerel, *Hydrometallurgy*, 57 (2000) 125.
8. W. Zhang, E. Ghali and G. Houlachi, *Mater. Technol.*, 29 (2014) A48.
9. F. Mohammadi, M. Tunnicliffe and A. Alfantazi, *J. Electrochem. Soc.*, 158 (2011) C450.
10. M. Mohammadi, R. P. Nogueira and A. Alfantazi, *Corrosion*, 72 (2016) 1181.
11. W. Zhang, M. Bounoughaz, E. Ghali and G. Houlachi, *Corros. Eng. Sci. Techn.*, 48 (2013) 452.
12. A. M. Lafront, W. Zhang, E. Ghali and G. Houlachi, *Electrochim. Acta*, 55 (2010) 6665.
13. R. H. Newnham, *J. Appl. Electrochem.*, 22 (1992) 116.
14. M. Nicol, C. Akilan, V. Tjandrawan and J. A. Gonzalez, *Hydrometallurgy*, 173 (2017) 178.
15. F. Hine, Y. Ogata and M. Yasuda, *Bull. Electrochem.*, 4 (1988) 61.
16. M. Clancy, C. J. Bettles, A. Stuart and N. Birbilis, *Hydrometallurgy*, 131–132 (2013) 144.
17. M. Stelter, H. Bombach and P. Saltykov, Corrosion behavior of lead-alloy anodes in metal winning, in *Sohn International Symposium Advanced Processing of Metals and Materials*, F. Kongoli and R. G. Reddy Editors, p. 451, Minerals, Metals & Materials Soc, Warrendale (2006).
18. R. J. Thibeau, C. W. Brown, A. Z. Goldfarb and R. H. Heidersbach, *J. Electrochem. Soc.*, 127 (1980) 1913.
19. L. Black, G. C. Allen and P. C. Frost, *Appl. Spectrosc.*, 49 (1995) 1299.
20. L. Burgio, R. J. H. Clark and S. Firth, *Analyst*, 126 (2001) 222.

21. T. Gao, H. Fjellvåg and P. Norby, *Anal. Chim. Acta*, 648 (2009) 235.
22. C. Julien, M. Massot, R. Baddour-Hadjean, S. Franger, S. Bach and J. P. Pereira-Ramos, *Solid State Ionics*, 159 (2003) 345.
23. N. Perez, Electrochemistry and Corrosion Science, Springer International Publishing, (2016).
24. A. Nidola, *Mater. Chem. Phys.*, 22 (1989) 183.
25. J. J. Lander, *J. Electrochem. Soc*., 98 (1951) 213.
26. J. J. McGinnity and M. J. Nicol, *Hydrometallurgy*, 144-145 (2014) 133.
27. C. Zhang, N. Duan, L. Jiang and F. Xu, *J. Electroanal. Chem.*, 811 (2018) 53.